Study of the Stagnating Flow in a Free Wake subjected to an Adverse Pressure Gradient

Wiebke Breitenstein[1]*, Peter Scholz[1]

[1]Technische Universität Braunschweig/Institute of Fluid Mechanics/Braunschweig, Germany

*w.breitenstein@tu-braunschweig.de

Abstract

The turbulent free wake is a well known shear flow. The flow properties are very complex, if subjected to an adverse pressure gradient (APG). Such a flow case is important for applied aerodynamics, because it occurs on multi-element high-lift airfoils at take-off and landing regimes. The longitudinal velocity in the wake decreases under APG, it can stagnate and even form a free turbulent recirculation bubble. Most turbulence models used in state-of-the-art numerical simulations significantly underpredict strength and size of this recirculation area.

This motivated to set up a high-quality validation case for the APG-wake problem. It consists of a flat plate, as a wake generator, and two pairs of symmetrically installed liner foils imposing an APG on the wake of the flat plate.

The paper presents the first results of the PIV measurements of this study. It includes the validation of the PIV measurement technique and a cross-comparison between results from stereoscopic and standard PIV for a Reynolds number based on the flat plate length (c = 1.058 m) of 1.6 million. The results provide good confidence that the experiment is well suited to generate good data for validation. The cross-comparison of two different PIV-configurations, 3C2D stereoscopic PIV and 2C2D standard PIV (with a finer resolution), will show a high similarity in the distributions of mean velocity and turbulent kinetic energy.

Nomenclature

c	chord-length of flat plate
Re	Reynolds number
k	turbulent kinetic energy
v	velocity
v_∞	freestream velocity
v_x, v_y, v_z	velocity component in streamwise, vertical and spanwise direction
X, Y, Z	coordinates in streamwise, vertical and spanwise direction

1 Introduction

The turbulent free wake is a well known shear flow that appears in many fluid mechanical problems. If the wake develops in a uniform flow, i.e. at zero pressure gradient, the near wake can be described by an analytical two-layer similarity approach, Alber (1980), and the far wake is actually a one-layer self-similar flow. The properties of the wake, however, become very complex, if it is subjected to an adverse pressure gradient (APG). Such a flow case is relevant for applied aerodynamics, because it occurs on multi-element high-lift airfoils at take-off and landing regimes: The wake of an upstream element (as the main wing) passes the APG introduced by an element located more downstream (as the flap). The longitudinal velocity in the wake decreases under APG and it is known that it can stagnate and even form a free turbulent recirculation bubble (in the mean sense), e.g. shown in the experimental setup of Driver & Mateer (2002). The maximum lift of a multi-element high-lift-airfoil can be limited due to such a free recirculation. However, most turbulence models used in state-of-the-art numerical simulations significantly underpredict strength and size of this recirculation area.

Recently, a high-quality validation case has been presented for the APG-wake problem, Guseva et al. (2018), Breitenstein et al. (2019). It consists of a flat plate as a wake generator and a symmetrical installed setup with two pairs of "liner foils", which act as a diffuser to generate the APG, as shown in Figure 1.
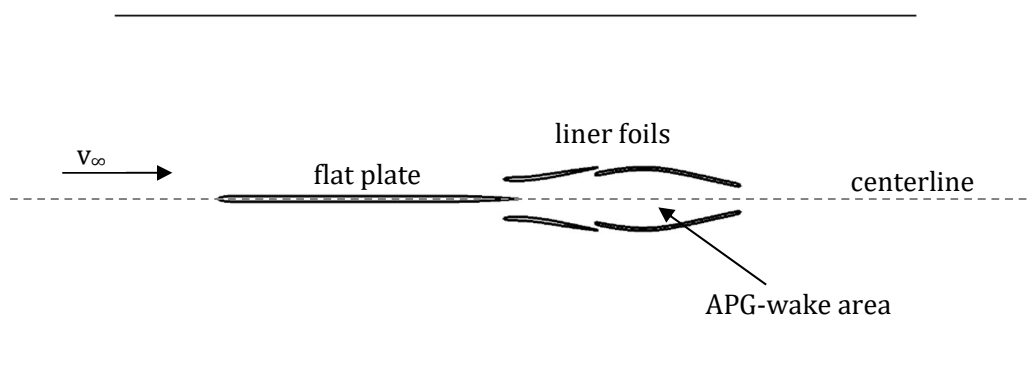

Figure 1: Overview of new validation case

This setup has been qualified with scale resolving simulations, Guseva et al. (2018). The setup itself and a comprehensive comparison of the basic properties, e.g. the pressure distributions along the elements, between experiment and numerical simulations can be found in Breitenstein et al. (2019). PIV measurements have been conducted in the X-Y-plane (in streamwise and vertical direction) in the center section of the setup using both, a stereoscopic 3C2D-configuration and a standard 2C2D-configuration. The stereoscopic setup was used to qualify the general characteristics of the flow field and estimate the statistical turbulence data as mean flow field (v_x, v_y, v_z) and turbulent kinetic energy. In the 2C2D-configuration a large focal length lens was used to achieve a high spatial resolution in the range of Taylor's micro scale λ_x.

This paper presents a first results of these PIV measurements and a cross-comparison between results from stereoscopic and standard PIV to validate the measurement technique for a Reynolds number based on the flat plate length (c = 1.058 m) of 1.6 million. This is done by the analysis of the estimated statistical turbulence data as mean flow field and turbulent kinetic energy. The paper is structured as followed: After this introduction the used experimental setup and the measurement

techniques are described. Section 3 presents the results from the PIV measurements including a validation of the turbulent statistics extracted from the PIV data and the comparison between stereoscopic and standard PIV.

2 Experimental Setup and Measurement Techniques

Model Elements

A schematic overview of the model elements in the test section of the wind tunnel is shown in Figure 2: It consists of a flat plate (FP), as a wake generator, and two pairs of symmetrically installed liner foils (LF1 and LF2) imposing an APG on the wake of flat plate. The gap between the upstream (LF1) and the downstream (LF2) liner foils allows a stronger APG without causing separation of the boundary layers on their surface. All the elements of the model (FP, LF1 and LF2) are mounted between the wind tunnel sidewalls. Windows on both sidewalls of the wind tunnel allow optical access to the wake area between the LFs for performing flow visualizations and PIV measurements.
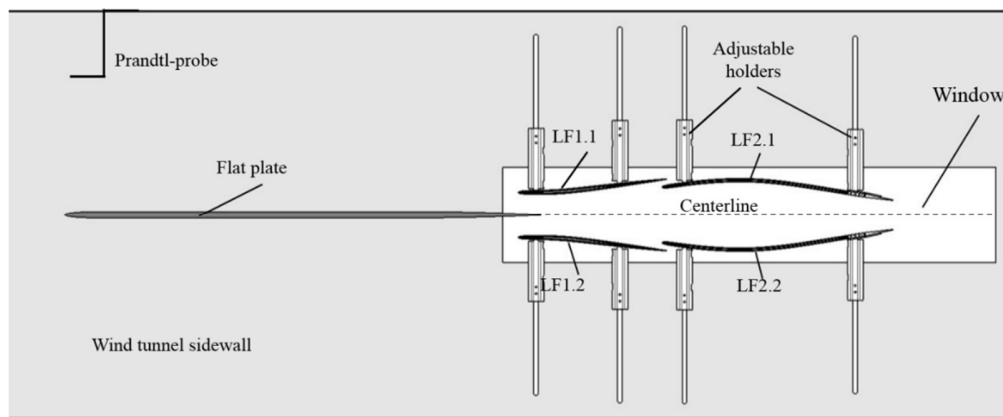

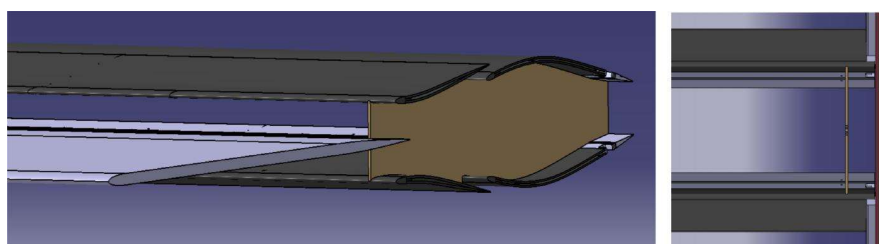Figure 2: Overview of model elements

Figure 3: Installation of splitter plates (the plates are actually transparent)

Additionally, two thin splitter plates were installed between the liner foils close to the tunnel walls (see Figure 3) to prevent the boundary layer of the wind tunnel side walls from separating due to the adverse pressure gradient caused by the liner foils. On the splitter plate, on the other hand, a new boundary layer is established which is more endurable against separation. This is fully described in Breitenstein et al. (2019). In order to allow the optical access to the flow field in the experimental setup the splitter plates are transparent. All detailed information regarding the aerodynamical design and the geometrical issues of the wind tunnel setup are also provided in Breitenstein et al. (2019).

Measurements Techniques

In this first entry the *X-Y*-plane (in streamwise and vertical direction) in the center section of the wind tunnel was investigated by using two different setups of PIV measurement: The stereoscopic 3C2D-configuration with a windows size of 160 mm x 100 mm gives evidence about the flow structure of the recirculation area including the statistical turbulence data as mean flow field and turbulent kinetic energy. For this, two cameras (*La Vision Imager Pro X*, 4008 x 2672 px, combined with a *La Vision PTU 10*) are installed on both sides of the wind tunnel in an angle of 45 degree regarding the *X-Y*-plane in the middle of the wind tunnel to enable a focused plane (see Figure 4). Panning the cameras in streamwise direction enables the investigation of the whole area of interest.
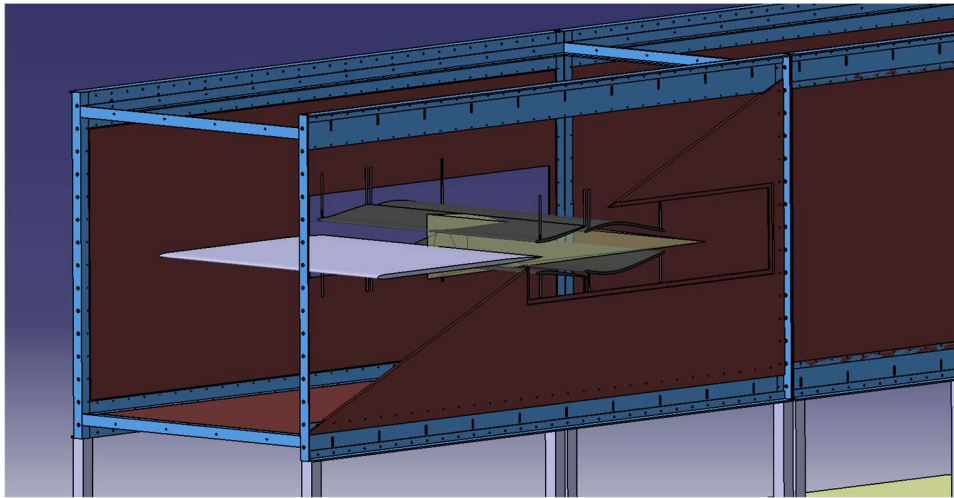

Figure 4: Experimental setup with stereo PIV

Different to this setup, investigations with the standard 2C2D-configuration using same cameras with a large focal length lens (window size 90 mm x 60 mm, shown in Figure 5) aim on the estimation of smaller turbulent length scales in the range of the Taylor micro scale λ_x. As in the stereoscopic 3C2D-configuration the investigation of the whole area of interest is achieved by panning the cameras in streamwise direction.
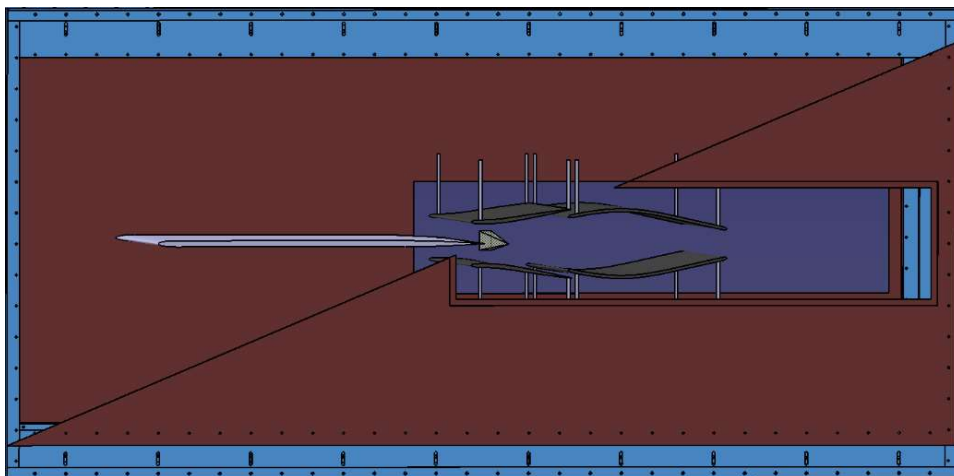

Figure 5: Experimental setup with standard PIV

In both setups a Nd:YAG double-pulse laser (*Quantel Evergreen 200 mJ*) was installed downstream of the experimental model under the wind tunnel floor. By deflection in two mirrors and passing the optic lenses the laser illuminates the *X-Y*-plane in the middle of the wind tunnel with a laser sheet. The laser sheet thickness was measured by using thermal paper at the trailing edge of the flat plate and different positions downstream: *X*=0 mm, *X*=370 mm and *X*=785 mm from trainling edge of the flat plate. This revealed a constant laser sheet thickness of approx. 3 mm. Hence, there was no need for adjusting the focal point when panning the cameras. DEHS seeding generated by three Laskin-nozzles was inserted well upstream of the settling chamber. The evaluation and analysis were done with *La Vision Davis 8.4*. The standard evaluation includes 1500 samples and a multi-pass algorithm with one pass in a 64x64 interrogation window and three passes in a 32x32 interrogation window. Beside PIV-measurements pressure distributions along all model elements and tuft videos were established to evidence the suitability of the experimental setup, Breitenstein et al. (2019).

Wind Tunnel Conditions

The tests are conducted in the low-speed closed-return wind tunnel at the Technische Universität Braunschweig (TU BS) with a square 1.3 m × 1.3 m cross section at the beginning of the test section which length is 6 m. To balance the increasing boundary layer displacement thickness the upper and lower wall of the test section are inclined by 0.2 degrees. The wind tunnel is ventilated to ambient pressure through openings at the very end of the test section (approximately 3.5 m downstream of all the installations). The temperature is controlled by a cooling system to a typical freestream temperature of around 37°C.

The wind tunnel can be operated at velocities from 15 to 60 m/s, which corresponds to variation the Reynolds number based on the flat plate length (c = 1.058 m) from 1 up to 4 million. The Reynolds number for the "design point" is 1.6 million, and additional tests are conducted at the Reynolds numbers 2.4 and 3.2 million, which are not considered in this paper.

3   Results

This chapter serves the presentation of the first PIV measurement results. It shows a short validation of the measurement technique and the post processing including the analysis of the number of samples and the uncertainty quantification of Wieneke (2015). Additionally, data from 2C2D-standard-PIV and 3C2D-stereo-PIV are presented and compared. For the analysis the mean velocity and the turbulent kinetic energy from the estimated statistical turbulence data were used.

This section gives an overview of the estimated velocities for standard and stereo PIV. Figure 6 shows the investigated area for both PIV configurations. Both configurations reveal the region of interest, the recirculation area. But the position differs a bit: it begins at *X*=0.36 m (standard), respectively *X*=0.39 m (stereo) and is larger in size in the standard PIV than in stereo PIV.

The distribution of streamwise velocity v_x along the centerline of wind tunnel and model (dashed line in Figure 6) shows that standard and stereo PIV have virtually the same results upstream of *X*=0.22 m. From this point on, as can be seen in Figure 7, the results from standard PIV tend to lower values in velocity, which results in an earlier appearance and larger area of recirculation. Outboard of the centerline (e.g. *Y*=0.02 m) the results for standard PIV are predicting higher velocities for *X*=0 m to X=0.1 m. As these areas are not of major interest and at the edge of the measurement field, the reasons for the offsets are not analysed in detail.
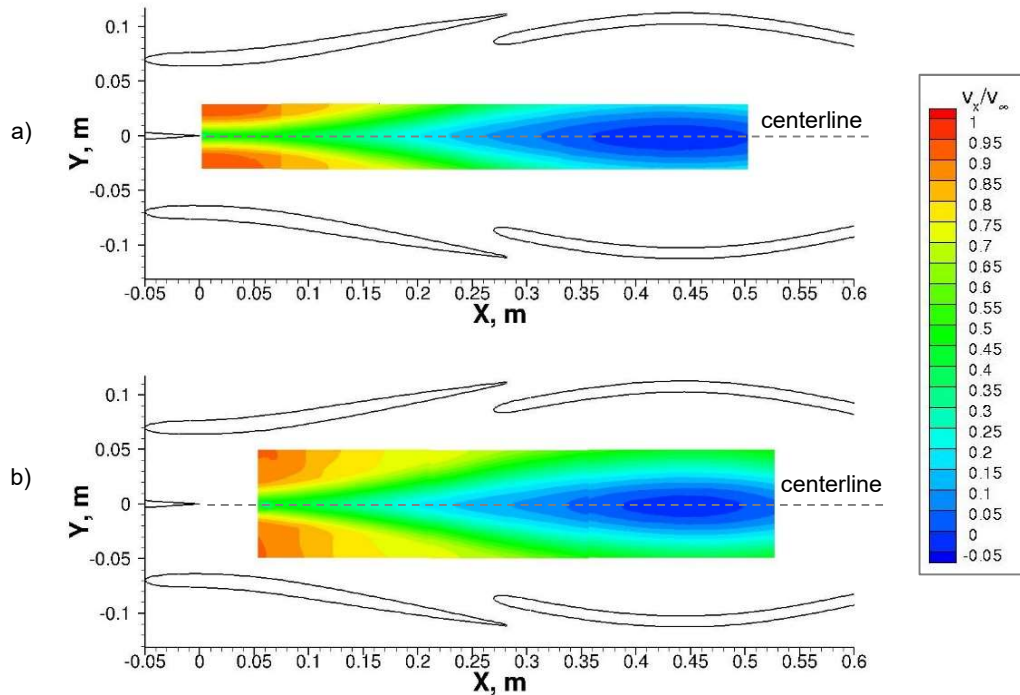
Figure 6: Overview of the investigated areas of standard PIV (a) and stereo PIV (b)
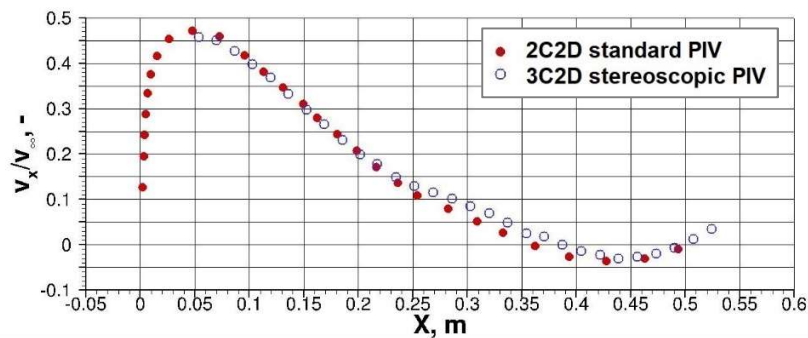

Figure 7: Velocity distribution in centerline

The study intends an estimation of the turbulence scales resolution in the range of Taylor's micro scale λ_x. Therefore, it is necessary to choose a more sensitive scale than the velocity for the validation. In this case we use the turbulent kinetic energy.

One important question of the evaluation is if enough samples were used to estimate turbulent statistical data. Figure 8 shows the distribution of the turbulent kinetic energy over increasing number of samples for two significant positions. One is at the beginning of the recirculation area in the centerline (0.4|0), which is one of the spots of main interest. The other one is positioned in the strongly sheared flow above this area where the gradient of the turbulent kinetic energy is higher (0.4|0.02). Results for 2C2D-standard-PIV (filled circles) and 3C2D-stereoscopic-PIV (unfilled circles) are given.
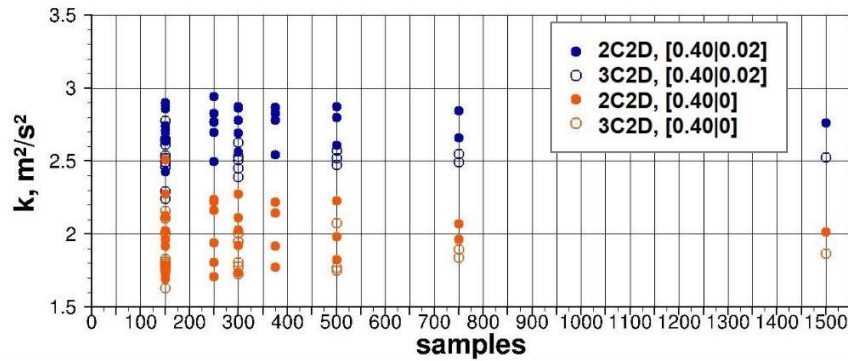
Figure 8: Deviation of turbulent kinetic energy depending on number of samples

The variation between the sets is significant, if the number of samples is small, it reduces constantly with higher number of samples. At 750 samples the deviation in turbulent kinetic energy is <±5% for both spots and PIV configurations. So, a number of 1500 samples should have an even lower error which is considered as adequate for standard and stereo PIV. Nevertheless, standard and stereo PIV differ in the absolute value of the turbulent kinetic energy for 1500 samples. One reason may be that for the 2C2D quasi-isotropic turbulence is assumed to estimate the third component of the TKE. Another reason may be the different physical size of the interrogation windows, which give different spatial filtering effects.

For the validation of additional uncertainties from the evaluation process the uncertainty quantification from Wieneke (2015) was conducted, which quantifies the effective accuracy of the image correlation process. Finally, the effective accuracy/uncertainty is interpreted as "noise" and subtracted from the turbulence values. The results for the turbulent kinetic energy along the centerline are given for both, standard and stereo PIV, in Figure 9. The figure compares data without uncertainty quantification ("raw data") and data with uncertainty quantification ("with uncertainty"). This reveals that the deviations predicted by the calculated uncertainties have a higher influence in the region up to X=0.25 m (up to 10%) and become lower towards the region with the recirculation area. This is presumably due to the increasing size of the small scale turbulence. In the following figures only data with uncertainty quantification are shown in order to consider the estimated uncertainties.
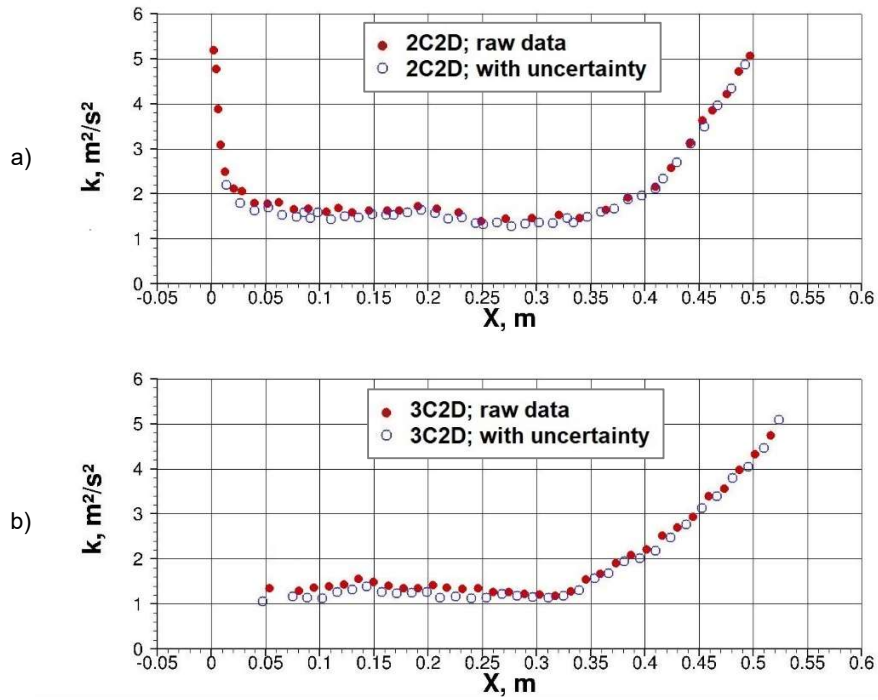
Figure 9: Deviation of uncertainty for 2C2D PIV (a) and for 3C2D PIV (b)

The comparison of 2C2D standard PIV and 3C2D stereoscopic PIV (Figure 10, Figure 11) shows high similarities in the distributions of turbulent kinetic energy in streamwise and vertical direction. The vertical distributions reveal the influence of the wake and the increasing of the turbulent kinetic energy in the whole profile along the X-direction. All in all, the standard PIV has a tendency to higher values in turbulent kinetic energy.
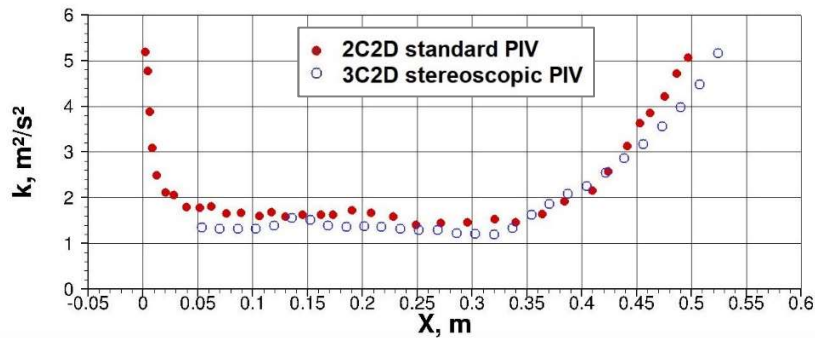

Figure 10: Distribution of turbulent kinetic energy in streamwise direction
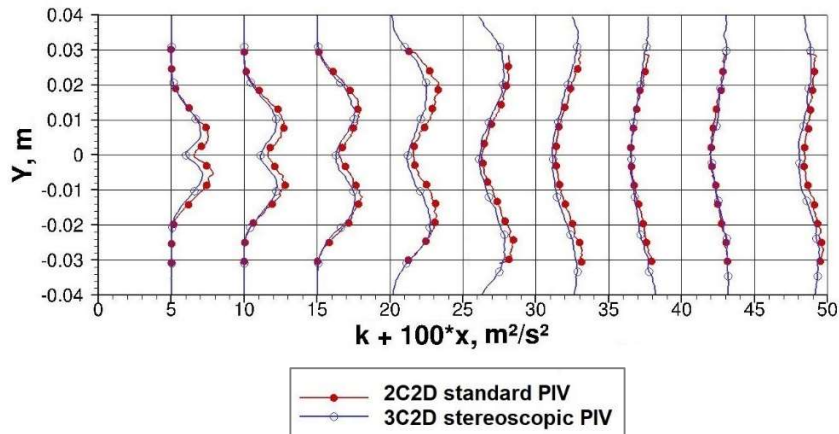
Figure 11: Distribution of turbulent kinetic energy in vertical direction

In a next step, but not part of the paper at hand, the measured turbulent kinetic energy will be compared to simulation (RANS / LES) results to conduct if the difference between the both measurement results are too large to justify the development and validation of enhanced turbulence models based on the presented results.

4   Conclusion

The paper provides results from the first PIV measurements of the investigation of a turbulent wake subjected to an adverse pressure gradient with a free turbulent recirculation area. The experimental model consists of a flat plate, which serves as the wake generator, and of two pairs of thin liner foils, which impose an adverse pressure gradient on the wake. In this first entry the investigations were conducted in the *X-Y*-plane (in streamwise and vertical direction) in the center section of the wind tunnel to give evidence about the flow structure of the wake and the recirculation area. The investigations included the statistical turbulence data as mean flow field and turbulent kinetic energy.

The paper additionally provides a basic validation of the measurement technique and the post processing including the analysis of the number of samples and the uncertainty quantification of Wieneke (2015). This analysis estimated the used number of samples (1500) as an adequate number of samples. The uncertainty quantification of Wieneke (2015) revealed uncertainties with a higher influence in the region up to X=0.25 m which became lower towards the region of the recirculation area, presumably, due to the increasing size of small scale turbulence.

Two different PIV-configurations, 3C2D stereoscopic PIV and 2C2D standard PIV (with a finer resolution), showed high similarities in the cross-comparison of distributions (mean velocity and turbulent kinetic energy). Smaller differences may result from the assumption of quasi-isotropic turbulence for 2C2D PIV and the different physical size of the interrogation windows, which give different spatial filtering effects.

In a next step differences between cases with variant pressure gradients and Reynolds numbers will be analyzed, and the experimental data will be cross-compared with the data extracted from scale-resolving simulations.

Acknowledgements

References

Alber, I.E. (1980) Turbulent Wake of a Thin, Flat Plate. *AIAA Journal* 18:1044-1051

Driver, D.M., Mateer, G.G. (2002) Wake flow in adverse pressure gradient. *International Journal of Heat and Fluid Flow* 23:564-571

Guseva, E., Shur, M., Strelets, M., Travin, A., Breitenstein, W., Radespiel, R., Scholz, P., Burnazzi, M., Knopp, T. (2018) Experimental/Numerical Study of Turbulent Wake in Adverse Pressure Gradient. In *7th Symposium on Hybrid RANS-LES Methods (HRLM), Berlin, Germany, September 17-19*

Breitenstein, W., Scholz, P., Radespiel, R., Burnazzi, M., Knopp, T., Guseva, E., Shur, M., Strelets, M. (2019) A Wind Tunnel Experiment for Symmetric Wakes in Adverse Pressure Gradients. In *AIAA Scitech* 2019:1875

Wieneke, B. (2015) PIV uncertainty quantification from correlation statistics, *Measurement Science and Technology* 26:074002